JOURNAL OF GEOPHYSICAL RESEARCH, VOL. 106, NO. A12, PAGES 29,305-29,312, DECEMBER 1, 2001

# Self-consistent model of solar wind electrons

V. Pierrard

Institut d'Aéronomie Spatiale de Belgique, Brussels, Belgium

M. Maksimovic

Observatoire de Paris, Département de Recherche Spatiale, Meudon, France

J. Lemaire

Institut d'Aéronomie Spatiale de Belgique, Brussels, Belgium

**Abstract.** We model the transformation of the steady state electron velocity distribution function in the collisional transition region of the solar wind by solving the Fokker-Planck equation. Alongside the proton and electron Coulomb collisions, effects of gravitational and electric and magnetic forces are also considered. The Coulomb collision term is calculated for any background velocity distribution function using a spectral method that we have developed and applied previously [*Pierrard et al.*, 1999]. Consistent treatment of electron self collisions is obtained using an iterative numerical method to match the velocity distribution functions of "test" and "background" electron distributions. Electron collisions with background solar wind protons are also taken into account. We find that Coulomb collisions have important effects on angular scattering of the electrons (i.e., on the pitch angle distribution) without changing their average density or mean radial temperature distribution. Finally, the importance of boundary conditions on the solution of the Fokker-Planck equation is discussed and emphasized.

## 1. Introduction

The solar wind is a plasma which is neither collision dominated nor completely collisionless. This means that neither the hydrodynamic approach based on the Euler or Navier-Stokes approximations nor the exospheric or pure collisionless approach is truly appropriate to model the expansion of plasma flow out of the hot solar corona. In this case the most appropriate method is solving the Fokker-Planck equation, which describes the evolution of the velocity distribution function (VDF) with radial distance from the Sun. The solution of the Fokker-Planck equation is especially important in the collisional transition region. Here, Coulomb collision effects between particles become less important with increasing height. We shall focus on an area of this region between 2 and 14 solar radii ($R_s$). The upper limit of 14 $R_s$ is where the mean free path of particles becomes larger than the density scale height. Additionally, both fluid and exospheric models place the acceleration region of the solar wind at low radial distances from the Sun.

Copyright 2001 by the American Geophysical Union.

Paper number 2001JA900133.
0148-0227/01/2001JA900133$09.00

In the last five years, interesting models have been developed to study the steady state electron VDF in the corona and at larger radial distances in the solar wind by solving the Fokker-Planck equation [*Lie-Svendsen et al.*, 1997; *Pierrard et al.*, 1999; *Lie-Svendsen and Leer*, 2000]. The models involve "test" electrons which, beside colliding with background particles, are submitted to the influence of external forces such as gravitational, electric, and Lorentz force. Up to now, only *Lie-Svendsen and Leer* [2000] took into account collisions with both background protons and electrons. In the present work both electron self collisions and collisions with protons are studied. Whereas earlier models were based on the hypothesis that the VDF of the background particles is a Maxwellian distribution, the present study adjusts the VDF of the background electrons to arrive at a self-consistent solution; that is, we impose that the VDF of the background and test electrons is the same.

It is important for the description of the solar wind that Coulomb collisions using the real VDF of the background particles are considered, rather than a nondisplaced Maxwellian approximation. Indeed, neglecting the bulk velocity of the background particles in the solar wind can modify the effects of the Coulomb collisions on the energy of the test electrons. To be self-consistent, we have assumed that the VDF of the background parti-

cles is the same as the VDF found by solving the Fokker-Planck equation. With an iterative process, we have obtained this solution using the model described in section 2. Section 3 describes the Coulomb collision term and the numerical method used to solve the Fokker-Planck equation. The results of the model are presented in section 4, and a discussion is given in section 5.

## 2. Description of the Model

The kinetic transport equation for the evolution of the velocity distribution function $f(\mathbf{r},\mathbf{v},t)$ for solar wind electrons is

$$\frac{\partial f(\mathbf{r},\mathbf{v},t)}{\partial t} + (\mathbf{v}\cdot\nabla_{\mathbf{r}})f(\mathbf{r},\mathbf{v},t) + (\mathbf{a}\cdot\nabla_{\mathbf{v}})f(\mathbf{r},\mathbf{v},t) = \left(\frac{df}{dt}\right)_c, \quad (1)$$

where $\mathbf{r}$ is the electron position, $\mathbf{v}$ is the electron velocity, $\mathbf{a}$ is the acceleration due to external forces, and $t$ is the time. We are interested in the steady state solution of this equation. In the case of the solar wind the external forces are gravitational, electric, and Lorentz force (the Lorentz force results from the magnetic field distribution).

The term $(df/dt)_c$ represents the effects of binary Coulomb collisions. By neglecting large-angle deflections, $(df/dt)_c$ can be represented by the Fokker-Planck collision operator [*Spitzer*, 1956; *Hinton*, 1983]

$$\left(\frac{df}{dt}\right)_c = -\frac{\partial}{\partial \mathbf{v}}\cdot\left[\mathbf{A}f(\mathbf{r},\mathbf{v},t) - \frac{1}{2}\frac{\partial}{\partial \mathbf{v}}\cdot(\mathbf{D}f(\mathbf{r},\mathbf{v},t))\right], \quad (2)$$

where $\mathbf{A}$ is the dynamic friction vector

$$\mathbf{A} = -4\pi\frac{Z_\alpha^2 Z_\beta^2 e^4 \ln\Lambda}{m_\alpha^2}\left(1+\frac{m_\alpha}{m_\beta}\right) \times \int d\mathbf{v}' f_\beta(\mathbf{v}')\frac{(\mathbf{v}-\mathbf{v}')}{(v-v')^3} \quad (3)$$

and $\mathbf{D}$ is the velocity diffusion tensor

$$\mathbf{D} = 4\pi\frac{Z_\alpha^2 Z_\beta^2 e^4 \ln\Lambda}{m_\alpha^2} \times \int d\mathbf{v}' f_\beta(\mathbf{v}')\left(\frac{\mathbf{I}}{v-v'} - \frac{(\mathbf{v}-\mathbf{v}')(\mathbf{v}-\mathbf{v}')}{(v-v')^3}\right). \quad (4)$$

In (3) and (4) the subscript $\alpha$ corresponds to the test electrons, $\beta$ corresponds to the background particles (i.e., electrons and protons), $\ln\Lambda$ is the usual Coulomb logarithm containing the Debye screening effect, $m$ is the mass, $Ze$ is the particle charge, and $f_\beta(\mathbf{v}')$ is the VDF of the background particles.

We assume azimuthal symmetry around the radial axis which is therefore parallel to the magnetic field direction and to the gravitational and electric forces. The magnetic field distribution $B(r)$ is assumed to be radial and varying as $r^{-2}$. As shown by *Pierrard et al.* [2001a], the introduction of a spiral magnetic field in a purely collisionless model modifies the temperature anisotropies but has minor influence on the other parameters. We are concerned here by stationary solutions of the Fokker-Planck equation. The velocity distribution is then a function of the radial distance $r$, the velocity $v$ and the function $\mu = \cos\theta$, where $\theta$ is the angle between the velocity vector and the radial direction.

The model development is described in full by *Pierrard et al.* [1999] and will not be repeated here in detail. Rather, we wish to emphasize an important improvement in the expression for the Coulomb collision term of a VDF of background particles.

## 3. General Collision Term for any Background Velocity Distribution Function

Previously, the Coulomb collision term has been calculated by considering that background particles VDF is a Maxwellian distribution [*Lie-Svendsen et al.*, 1997] (or a more general Kappa function in the work of *Pierrard et al.* [1999]). However, the VDF of background particles is actually very different from being Maxwellian. For example, an isotropic Maxwellian distribution has a bulk velocity of zero, when, in truth, the background particles are not static but move in the solar wind with a large bulk velocity. However, the assumption of a Maxwellian distribution was nevertheless used since it simplified the expression of the Coulomb collision term, allowing it to be calculated analytically [*Hinton*, 1983].

In this work we present the general expression of the Coulomb collision term without assumption on the background distribution. Since the spectral method developed by *Pierrard et al.* [1999] to solve the Fokker-Planck equation also allows evaluation of integrals, the Coulomb collision term can be calculated for any given background distribution. Distributions can be taken from observations or from earlier models. The Coulomb collision terms must be added for each species colliding with the test electrons. Here, we will consider collisions with background electrons and protons, which constitute the major particles in the solar wind.

Using spherical coordinates, the Coulomb collision term is given as [*Rosenbluth et al.*, 1957; *Delcroix and Pers*, 1994]

$$x^2\left(\frac{df}{dt}\right)_c = 2\pi\frac{Z_\alpha^2 Z_\beta^2 e^4 \ln\Lambda}{m_\alpha^2} \left[\frac{\partial}{\partial x}\left(f\left\{-2x^2(1+\frac{m_\alpha}{m_\beta})\frac{\partial h}{\partial x}\right.\right.\right.$$

$$
\begin{aligned}
&- 2\frac{\partial g}{\partial x} + 2\frac{\mu}{x}\frac{\partial g}{\partial \mu} - \frac{1-\mu^2}{x}\frac{\partial^2 g}{\partial \mu^2}\Big\}\Big) \\
&+ \frac{\partial}{\partial \mu}\Big(f\Big\{ - 2(1-\mu^2)(1+\frac{m_\alpha}{m_\beta})\frac{\partial h}{\partial \mu} \\
&+ \frac{2\mu}{x}\frac{\partial g}{\partial x} - \frac{2}{x^2}\frac{\partial g}{\partial \mu} \\
&+ 2\frac{(1-\mu^2)}{x}\frac{\partial^2 g}{\partial x \partial \mu} + \frac{\mu(1-\mu^2)}{x^2}\frac{\partial^2 g}{\partial \mu^2}\Big\}\Big) \\
&+ \frac{\partial^2}{\partial x^2}\Big(f\Big\{x^2\frac{\partial^2 g}{\partial x^2}\Big\}\Big) \\
&+ \frac{\partial^2}{\partial x \partial \mu}\Big(2f(1-\mu^2)\Big\{\frac{\partial^2 g}{\partial x \partial \mu} - \frac{1}{x}\frac{\partial g}{\partial \mu}\Big\}\Big) \\
&+ \frac{\partial^2}{\partial \mu^2}\Big(f\Big\{\frac{(1-\mu^2)}{x}\frac{\partial g}{\partial x} - \frac{\mu(1-\mu^2)}{x^2}\frac{\partial g}{\partial \mu} \\
&+ \frac{(1-\mu^2)^2}{x^2}\frac{\partial^2 g}{\partial \mu^2}\Big\}\Big)\Big], \qquad (5)
\end{aligned}
$$

$$
h(x,\mu) = \int \frac{f_\beta(r,x',\mu')}{|\mathbf{x}-\mathbf{x}'|}d\mathbf{x}', \qquad (6)
$$

$$
g(x,\mu) = \int f_\beta(r,x',\mu')|\mathbf{x}-\mathbf{x}'|d\mathbf{x}', \qquad (7)
$$

where $x$ is the dimensionless velocity,

$$
x = \sqrt{\frac{m_\beta}{2kT_\beta}}v = \frac{v}{w_\beta}. \qquad (8)
$$

### 3.1. Expansion in Legendre Polynomials

The VDF of the background particles can be expanded as a series of Legendre polynomials

$$
f(x,\mu) = \sum_{n=0}^{\infty} a_n(x)P_n(\mu). \qquad (9)
$$

Consequently, (6) and (7) can be expressed as [*Rosenbluth et al.*, 1957]

$$
h(x,\mu) = \sum_{n=0} A_n(x,\mu)P_n(\mu), \qquad (10)
$$

with

$$
\begin{aligned}
A_n(x,\mu) = \frac{4\pi}{2n+1}\Big[&\int_0^x dx'\frac{(x')^{n+2}}{x^{n+1}}a_n(x') \\
&+ \int_x^\infty dx'\frac{x^n}{(x')^{n-1}}a_n(x')\Big], \qquad (11)
\end{aligned}
$$

$$
g(x,\mu) = \sum_{n=0} B_n(x)P_n(\mu), \qquad (12)
$$

with

$$
\begin{aligned}
B_n(x) = -\frac{4\pi}{4n^2-1}&\Big[\int_0^x dx' a_n(x')\frac{(x')^{n+2}}{x^{n-1}}\Big(1 - \frac{n-\frac{1}{2}(x')^2}{n+\frac{3}{2}x^2}\Big) \\
&+ \int_x^\infty dx' a_n(x')\frac{x^n}{x'^{n-3}}\Big(1 - \frac{n-\frac{1}{2}x^2}{n+\frac{3}{2}(x')^2}\Big)\Big]. \qquad (13)
\end{aligned}
$$

### 3.2. Advantage of the Spectral Method

The Fokker-Planck equation is solved using a spectral method developed initially for the polar wind [*Pierrard and Lemaire*, 1998]. It was later adapted for use for the solar wind [*Pierrard et al.*, 1999, 2001b]. When the VDF of the background particles is known, the collision term integrals can be calculated easily by expanding the solution in terms of orthogonal polynomials,

$$
\begin{aligned}
f(z,x,\mu) = \exp(-x^2)\times &\\
\Big(\sum_{l=0}^{n-1}\sum_{s=0}^{N-1}\sum_{m=0}^{M-1} a_{lsm}P_l(\mu)S_s(x)L_m(z)\Big), &\qquad (14)
\end{aligned}
$$

where $P_l(\mu)$ are Legendre polynomials, $S_s(x)$ are speed polynomials, and $L_m(z)$ are displaced Legendre polynomials with $\sigma(r) = 2\pi Z_\alpha^2 Z_\beta^2 e^4 \ln\Lambda/[2kT_\beta(r))]$ and $z = \int_{r_0}^R \sigma(r)n_\beta(r)dr$.

Integrals (6) and (7) can be calculated by Gauss quadrature,

$$
\int_a^b W(y)G(y)dy \simeq \sum_{i=0}^{N-1} w_i G(y_i), \qquad (15)
$$

where $y_i$ are the $N$ roots of the $N$th order polynomial $Q_N(y)$ of the set orthogonal with weight function $W(y)$, $G(y_i)$ are the values of the function $G(y)$ at the quadrature points, and $w_i$ are weights associated with the function $W(y)$. In the discrete ordinate basis the derivatives of any continuous function $f(y)$ can similarly be approximated by expansions

$$
\Big(\frac{\partial f}{\partial y}\Big)_{y=y_i} \simeq \sum_{j=0}^{N-1} D_{ij}f(y_j), \qquad (16)
$$

where $D_{ij}$ are the matrix elements of the derivative operator in the polynomial basis [*Shizgal and Blackmore*, 1984].

### 3.3. Isotropic Background Distribution

When the background functions are isotropic (i.e., $\partial f_\beta/\partial\mu = 0$), the Coulomb collision term (equation (5)) becomes

$$
\begin{aligned}
\Big(\frac{df}{dt}\Big)_c = \sum_\beta 2\pi\frac{Z_\alpha^2 Z_\beta^2 e^4 \ln\Lambda}{m_\alpha^2} &\\
\Big[\frac{2}{x^2}\frac{\partial g}{\partial x}\frac{\partial f}{\partial x} + \frac{\partial^2 g}{\partial x^2}\frac{\partial^2 f}{\partial x^2} + f\Delta^2 g &\\
+ \frac{1}{x^3}\frac{\partial g}{\partial x}\frac{\partial}{\partial \mu}(1-\mu^2)\frac{\partial f}{\partial \mu} + 2\frac{\partial f}{\partial x}\frac{\partial \Delta g}{\partial x} &
\end{aligned}
$$

$$- \; 2\left(1+\frac{m_\alpha}{m_\beta}\right)\left(f\Delta h+\frac{\partial h}{\partial x}\frac{\partial f}{\partial x}\right)\Bigg], \quad (17)$$

where $\Delta$ is the Laplacian

$$\Delta = \frac{\partial^2}{\partial x^2}+\frac{2}{x}\frac{\partial}{\partial x}+\frac{1}{x^2}\frac{\partial}{\partial \mu}(1-\mu^2)\frac{\partial}{\partial \mu}, \quad (18)$$

$$h = \int_0^{2\pi} d\phi \int_{-1}^{1} d\mu' \int_0^{\infty} dx' x'^2 \frac{f_\beta(r,x',\mu')}{\sqrt{x^2+x'^2-2xx'\mu'}}, \quad (19)$$

$$g = \int_0^{2\pi} d\phi \int_{-1}^{1} d\mu' \int_0^{\infty} dx' x'^2 f_\beta(r,x',\mu') \sqrt{x^2+x'^2-2xx'\mu'}. \quad (20)$$

When the background particles have a Maxwellian VDF, important simplifications lead to the generally used expression of the collision term [*Hinton*, 1983], as used in the model developed by *Pierrard et al.* [1999].

## 4. Assumptions for the Background Particles

As a consequence of the VDF of the background and test electrons being identical (section 1), the Fokker-Planck equation is nonlinear. As this can present substantial difficulties in its evaluation, the VDF of the background particles and test electrons are treated somewhat differently.

### 4.1. Electron-Electron Self Collisions

For electron-electron self collisions (neglecting electron-proton collisions) the VDF of the test and background electron distributions are treated consistently by employing an iterative numerical method.

Firstly, the Fokker-Planck equation is solved using a local isotropic Maxwellian distribution for the background electrons VDF, like in the work of *Pierrard et al.* [1999]. The density and temperature of the background particles vary with radial distance. The background density and temperature profiles used for the model are obtained from the exospheric Lorentzian model described by *Maksimovic et al.* [1997a], with a value of kappa=100. With such a large value of the kappa index, the generalized Lorentzian VDF is similar to a Maxwellian VDF. The electric potential difference which accelerates the solar winds electrons and protons is also taken from this exospheric model.

Secondly, the VDF of the test electrons, found by solving the Fokker-Planck equation, is used for the background distribution VDF. The Fokker-Planck equation is solved again with this new assumption on the background electrons. The process is then iterated so that the solution, i.e., the test electron distribution, corresponds to the background electron distribution. The iterative process converges quickly as the low-energy electrons have a VDF which is practically isotropic and Maxwellian.

Of great importance are the boundary conditions which determine the flux and the spatial evolution of the VDF. *Pierrard et al.* [1999] take the boundary conditions as typical electron VDFs observed at 1 AU. This was then used to determine the VDF at other radial distances. In the present work, separate boundary conditions are employed at the inner and outer limits of 2 and 14 $R_s$ in order to model the collisional transition region. At the lower boundary where the plasma is dominated by Coulomb collisions the upward part of the electron VDF is taken as Maxwellian with a temperature $T_e = 1.5 \times 10^6$ K and a density $n_e = 3 \times 10^{11}$ m$^{-3}$. At the upper boundary where Coulomb collisions become less important the boundary condition employed is that no incoming electrons exist with a velocity greater than the escape velocity $v_{esc}$:

$$f(2\ R_s, v, \mu > 0) = n_e\left(\frac{m_e}{2\pi k T_e}\right)^{3/2} \exp(-m_e v^2/2kT_e), \quad (21)$$

$$f(14\ R_s, v > v_{esc}, \mu > 0) = 0, \quad (22)$$

$$f(14\ R_s, v < v_{esc}, \mu) = f(14\ R_s, v < v_{esc}, -\mu). \quad (23)$$

The upper boundary condition is based on the premise employed in exospheric models, i.e., since collisions be-

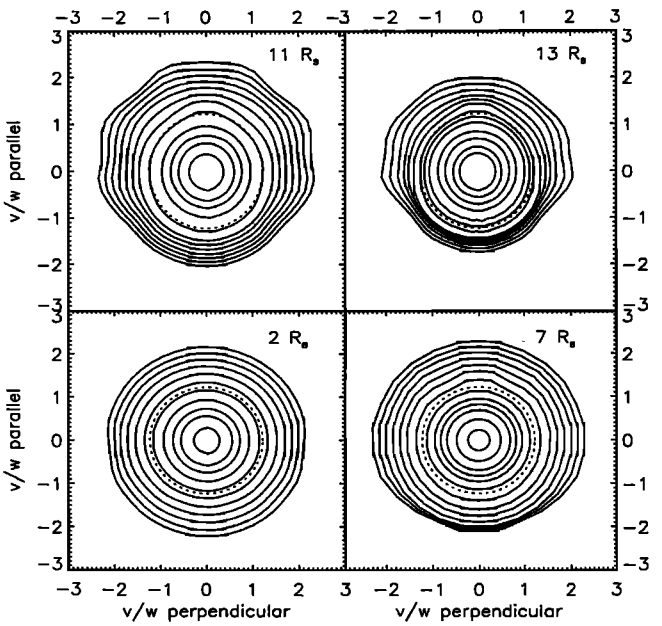


**Figure 1.** Isocontours of the electron velocity distribution function (VDF) for four different radial distances. Isocontours were generated using a collisional model based on the solution of the Fokker-Planck equation with an upper and lower boundary condition, Coulomb collisions and identical VDFs for the background and test electrons (electron-proton collisions are neglected). The dotted circle represents the normalized thermal velocity with $w = \sqrt{m_e/2kT_0}$.

come negligible for high-energy particles above 14 $R_s$, electrons with $v > v_{esc}$ can never return. Condition (22) forces the distribution to become non-Maxwellian and has a direct influence on the flux value. At 14 $R_s$ the value of the escape velocity is $x_{esc} = 1.73$, i.e., $v_{esc} = 1.166 \times 10^4$ km s$^{-1}$. Note that both the upper and lower boundary conditions are accepted as "standard".

### 4.2. Results of Electron-Electron Self Collisions

Figure 1 shows isocontours of the electron VDF for four different radial distances. The transformation of the VDF from nearly Maxwellian at the lower boundary to an anisotropic distribution at the upper boundary is clearly visible. The flux is due to high-energy electrons, which is a direct consequence of boundary condition (23) which imposes specular reflection at the upper level and implies that the core electrons (in this case electrons with an energy less than the escape energy) do not contribute to the net flux or the energy flux. This hypothesis is justified as it would be expected that collisions between low-energy electrons maintain an almost isotropic distribution. In addition, low-energy electrons are coupled to the background electrons by Coulomb collisions while high-energy electrons escape quasi-freely.

That the flux consists solely of high-energy electrons is in line with exospheric theory (which was used to determine the upper boundary condition). This is fundamentally different from the fluid description where particles of all energies contribute to the flux (and flow with the same velocity). Nevertheless, in the case of solar wind electrons where the thermal velocity is much larger than the bulk velocity it is difficult to establish from measured VDFs which of these theories gives the best description of the electron VDF.

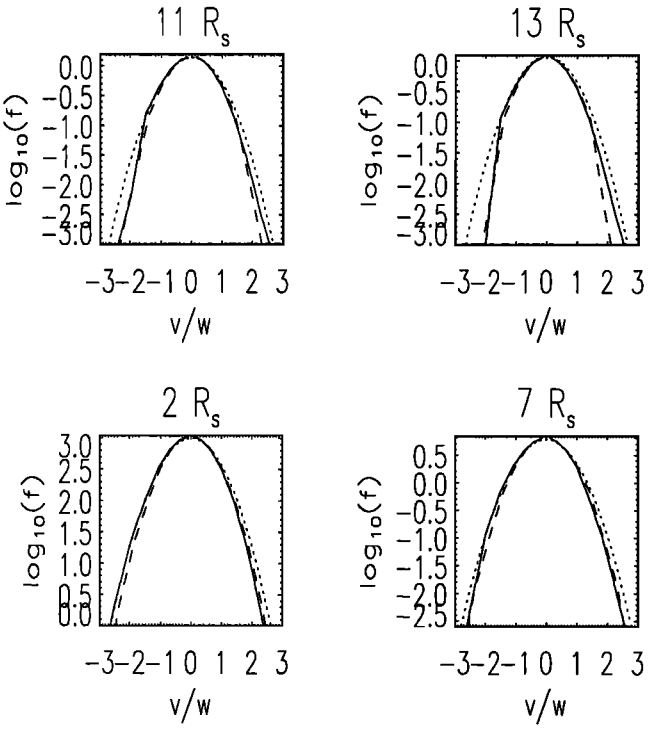


**Figure 2.** Vertical cuts through the VDF $f$ of Figure 1. The solid line is $f(v_\parallel/w)$, and the dashed line is $f(v_\perp/w)$. The Maxwellian velocity distribution function is represented by the dotted line.

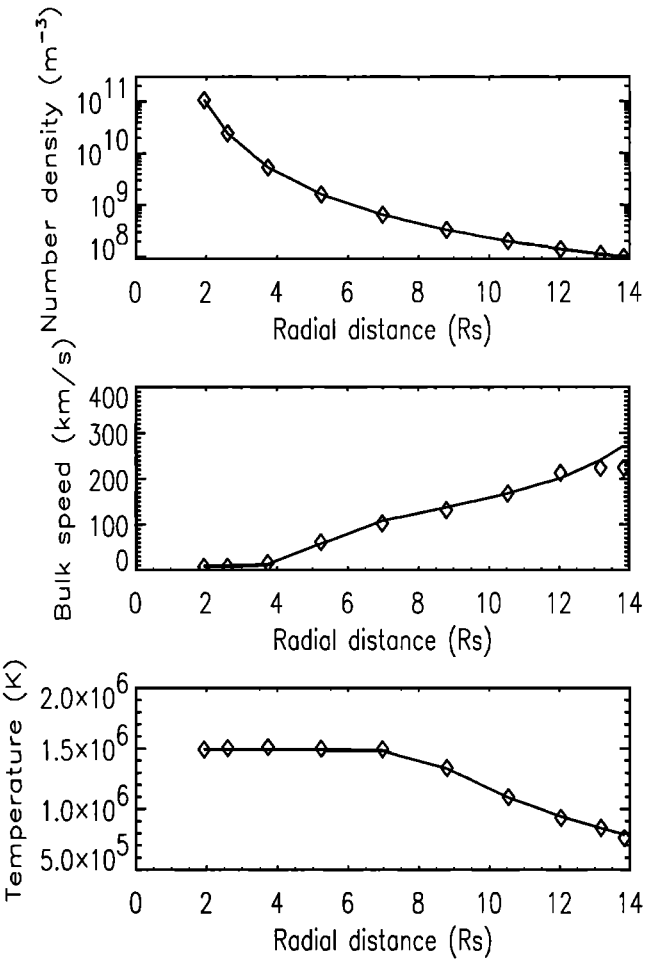


**Figure 3.** Density, bulk velocity, and temperature profiles between 2 and 14 $R_s$. Diamonds show collisional model with electron-proton collisions neglected, and solid lines are when electron-proton collisions are included.

Figure 2 shows vertical cuts through the VDF $f$ (solid line showing $f$ as a function of $y_\parallel$ and dashed line showing $f$ as a function of $y_\perp$). Assuming a Maxwellian VDF at the lower boundary, the model does not lead to a halo population at large radial distance, i.e., an enhancement of high-energy electrons (as is observed in the solar wind). Also, the nearly isotropic halo observed in the solar wind is not reproduced, particularly in the perpendicular direction (nor is it reproduced in the model of *Lie-Svendsen and Leer* [2000], which uses the same boundary conditions).

With the chosen boundary conditions (in particular with (21)) it is not possible to obtain at large radial distance VDFs which decrease in all directions as a power law of the velocity (rather they decrease exponentially). Nevertheless, a halo population is observed at large radial distances in the solar wind electron distributions in both parallel and perpendicular directions.

A halo population at large radial distance can be obtained by assuming its existence at the lower boundary (condition (21)). This can be achieved by using a generalized Lorentzian rather than Maxwellian distribution [*Pierrard and Lemaire*, 1996; *Maksimovic et al.*, 1997a]. Alternatively, when suprathermal tails are introduced low in the corona, their importance increasing with radial distance due to the velocity filtration process [*Scudder*, 1992; *Pierrard et al.*, 1999; *Meyer-Vernet*, 2001], a halo population at large radial distance is obtained which fits well with observed distributions. Finally, such a halo population can be created by adding other possible processes, such as wave-particle interactions, to the external forces and collisions.

Figure 3 (shown as diamonds) shows the radial profiles of density, bulk velocity, and temperature obtained by the model between 2 and 14 $R_s$. The density and temperature (and other even momentums) are sensitive to the background assumptions detailed at the beginning of section 4.1. The bulk velocity and flux (and other odd momentums) are more dependent on the boundary conditions. Note that results at the upper boundary would be in good agreement with equivalent results using an exospheric model (the exospheric model can be used to obtain profiles of average macroscopic quantities at radial distances above the transition region considered here).

### 4.3. Adding Electron-Proton Collisions

In adding Coulomb collisions with protons to the electron-electron collisions detailed above, *Lie-Svendsen and Leer* [2000] assumed that the VDF of the background protons is an isotropic Maxwellian distribution with a bulk velocity of zero. Since this is contrary to observations that the bulk velocity of background protons is nonzero, our model assumes that the background proton VDF is a displaced Maxwellian with a bulk velocity $u$ (the bulk velocity was obtained from a exospheric Lorentzian model).

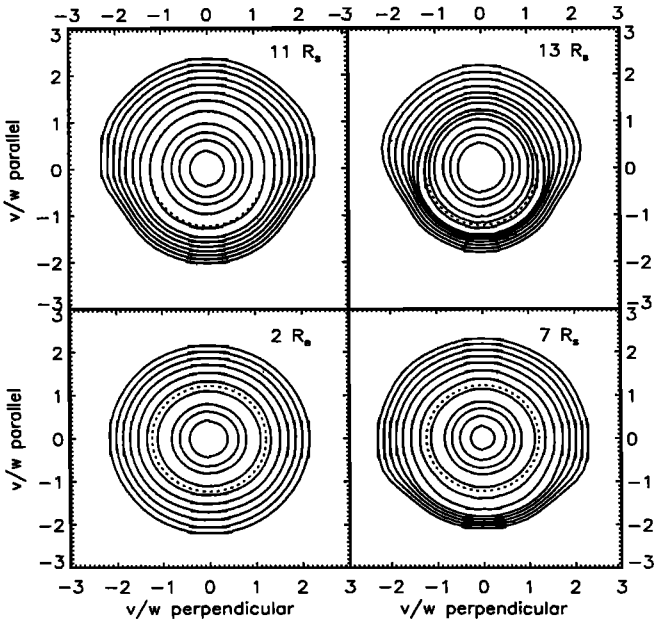


**Figure 4.** Isocontours of the electron VDF for four different radial distances. Isocontours were generated using a collisional model based on the solution of the Fokker-Planck equation with an upper and lower boundary condition and Coulomb collisions involving background electrons and protons.

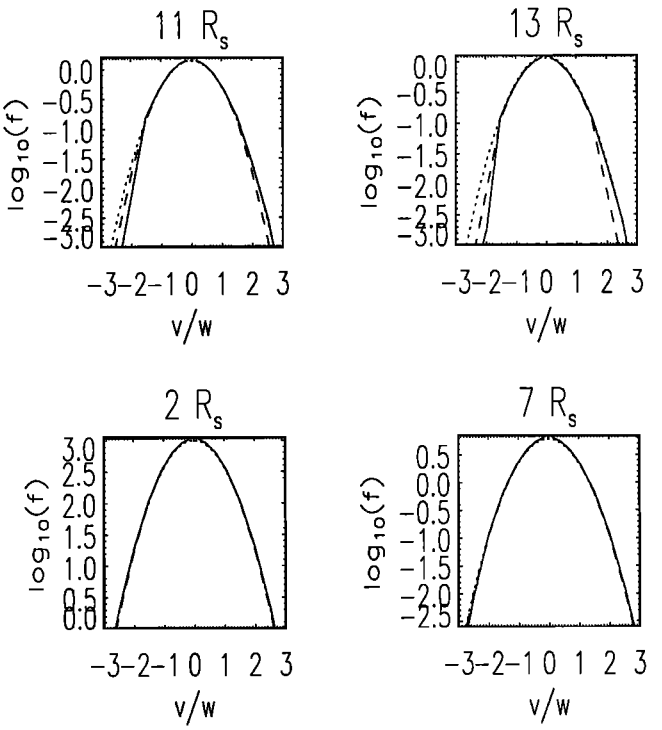


**Figure 5.** Vertical cuts through the VDF $f$ of Figure 4. The solid line is $f(v_\parallel/w)$, and the dashed line is $f(v_\perp/w)$. Electron-proton collisions are included.

### 4.4. Results When Including Electron-Proton Collisions

Figures 4 and 5 are as Figures 1 and 2, except computed using the collisional model with both electron-electron and electron-proton collisions. (Figure 4 shows isocontours of the electron VDF, and Figure 5 shows vertical cuts through the VDF $f$). Comparing Figures 4 and 5 with Figures 1 and 2, it is seen that including the proton collisions slightly modifies the electron diffusion.

Figure 3 shows the radial profiles of density, bulk velocity, and temperature obtained when electron-proton collisions are included with electron-electron collisions (solid line). Comparing with the electron-electron collision results discussed earlier (shown as diamonds), all three profiles are weakly affected. In the transition region the temperature anisotropy remains very weak. At larger radial distance the collisional model gives temperature anisotropy around 1.3. Purely exospheric models give too high temperature anisotropies ($> 1.3$) because collisions are neglected. This indicates that the inclu-

sion of Coulomb collisions is significant in the diffusion of particles.

## 5. Discussion

The Fokker-Planck equation has been solved within the collisional transition region between 2 and 14 $R_s$, allowing the transformation of electron VDFs in this key region of solar wind acceleration to be modeled. The model included both external forces and Coulomb collisions with electrons and protons. On applying this model, we found the following:

1. The mean even moments of the VDF are affected only slightly by Coulomb collisions. The density and mean temperature profiles obtained using the collisional model are very similar to equivalent results obtained using the exospheric model.

2. Coulomb collisions involving electrons and protons have an important effect on the pitch angle of scattered electrons. This is visible in Figures 1 and 4, which present isocontours of electron VDFs. Using the collisional model, the electron temperature anisotropy is weaker (remaining close to 1) than that produced using the exospheric model (can reach a value greater than 10).

3. The bulk velocity is mainly determined by the upper boundary condition (22), thus truncating the electron VDF. Boundary condition (23), which imposes specular reflection, implies that core electrons do not contribute to the bulk velocity. It is important to note that the boundary conditions are therefore essential in the collisional model and are also responsible for differences obtained when comparing it with a fluid model. However, since the thermal velocity is much greater than the bulk velocity, the bulk velocity of the core electrons is difficult to observe. Therefore fluid and exospheric models give similar values of average macroscopic quantities.

4. Owing to the electron thermal velocity being much greater than the bulk velocity, and from the presence of low-energy photoelectrons, solar wind observations can not be used to determine whether the electron core population is centered on zero (as is the case of completely collisionless models) or centered on the velocity of the solar protons (as is the case of collision-dominated plasma models). Nevertheless, observations seem to indicate that the core electrons have a bulk velocity lower than that of the solar wind [*Feldman et al.*, 1975]. This is true for the slow-speed solar wind (around 50 km $s^{-1}$), while for the high-speed solar wind (around 150 km $s^{-1}$) the difference is even greater.

5. Owing to the solar wind having a low density, Coulomb collisions are most important at low radial distances where the bulk velocity is relatively small. This explains why the heat flux found in exospheric models is in good agreement with observations [*Lemaire and Scherer*, 1971, 1973].

6. The main contributions to the velocity and energy flux are from high-energy electrons which have escaped practically collisionless from the solar corona. Fluid models are useful in providing a "limiting case" for the collision-dominated regime, while exospheric models provide a similar value for the collisionless regime. A good transition region model must account for both low-energy electrons which are affected by Coulomb collisions and high-energy electrons which can escape quasi-freely.

7. The electron and proton bulk velocities are equal. This is due not only to collisional equilibrium but also from the quasi-neutrality of the plasma. Though at large radial distances, where Coulomb collisions are less important, the proton and electron fluxes become equal because no net current is transported by the solar wind. Note that the heavier ions in the fast solar wind have different bulk velocities and at large radial distance are not in collisional equilibrium.

8. In exospheric models the "core" corresponds to the relatively cool population which is trapped within the ambipolar thermoelectric potential well of the heliosphere ($\phi_E$), whereas the "halo" and "strahl" are composed of electrons energetic enough to escape this potential. The strongly anisotropic strahl component can be understood as the result of conservation of magnetic moment along the magnetic field line. Core and strahl populations of electrons are reproduced by the collisional model. However, the fact that the halo component is very isotropic in the observed VDFs is not completely understood [*Maksimovic et al.*, 1997b]. Indeed, both in results presented here and in those of *Lie-Svendsen and Leer* [2000], the halo component is not present in the parallel antisunward direction for velocities greater than the local escape velocity (which is roughly equal to $\sqrt{2e\phi_E/m_e}$). Also, the suprathermal tails corresponding to the halo population are not obtained in the perpendicular direction when a Maxwellian distribution is assumed at the lower boundary level. Additionally, the angular dispersion due to Coulomb collisions is not sufficient to diffuse the strahl in all directions. This is quite logical since Coulomb collisions have a minimal effect on high-energy electrons (due to the sharp dependence of the Coulomb cross section with the velocity of the particles).

9. The two-temperature electron distributions often observed in the solar wind are not produced in the perpendicular direction when a Maxwellian distribution is assumed at the lower boundary layer. This suggests that the electron population might be already enhanced by suprathermal particles in the corona. Indeed, in the model, halo electrons are obtained at large radial distances only when a Lorentzian VDF is imposed at the lower boundary level [*Pierrard et al.*, 1999]. The velocity filtration effect amplifies the high-energy suprathermal tails if they exist in the corona but does not create them. The origin of the halo population in the corona therefore remains undetermined. However, in any case, it can be associated with the low temperature of the

coronal holes where the high-speed solar wind is issued and where high-energy suprathermal tails are most often observed. Another possibility is the presence of other physical processes which have not been included in our model which might influence the transformation of VDFs in the transition region.

**Acknowledgments.** This work has been supported at the Belgian Institute for Space Aeronomy by the Service des Affaires Scientifiques, Techniques et Culturelles and the Fonds National de la Recherche Scientifique, under grant FC 36556. Discussions with H. Lamy and N. Meyer-Vernet are acknowledged.

Michel Blanc thanks Egil Leer for his assistance in evaluating this paper.

## References

Delcroix, J.-L., and A. Pers, *Physique des Plasmas*, 2, Savoirs Actuels, InterEditions/CNRS Editions, 499 pp., Paris, 1994.

Feldman, W. C., J. R. Asbridge, S. J. Bame, M. D. Montgomery, and S. P. Gary, Solar wind electrons, *J. Geophys. Res., 80*, 4181, 1975.

Hinton, F. L., Collisional transport in plasma, in *Basic Plasma Physics I and II*, edited by A. A. Galeev and R. N. Sudan, pp. 148-200, North-Holland, New York, 1983.

Lemaire, J., and M. Scherer, Kinetic models of the solar wind, *J. Geophys. Res., 76*, 7479, 1971.

Lemaire, J., and M. Scherer, Kinetic models of solar and polar winds, *Rev. Geophys., 11*, 427, 1973.

Lie-Svendsen, O., and E. Leer, The electron velocity distribution in the high-speed solar wind: Modeling the effects of protons, *J. Geophys. Res., 105*, 35, 2000.

Lie-Svendsen, O., V. H. Hansteen, and E. Leer, Kinetic electrons in high-speed solar wind streams: Formation of high-energy tails, *J. Geophys. Res., 102*, 4701, 1997.

Maksimovic, M., V. Pierrard, and J. Lemaire, A kinetic model of the solar wind with Kappa distributions in the corona, *Astron. Astrophys., 324*, 725, 1997a.

Maksimovic, M., V. Pierrard and P. Riley, Ulysses electron distributions fitted with Kappa functions, *Geophys. Res. Lett., 24*, 1151, 1997b.

Meyer-Vernet, N., Large scale structure of planetary environments: The importance of not being Maxwellian, *Planet. Space Sci., 49*, 247, 2001.

Pierrard, V., and J. Lemaire, Lorentzian ion exosphere model, *J. Geophys. Res., 101*, 7923, 1996.

Pierrard, V., and J. Lemaire, A collisional kinetic model of the polar wind, *J. Geophys. Res., 103*, 11,701, 1998.

Pierrard, V., K. Issautier, N. Meyer-Vernet and J. Lemaire, Collisionless solar wind in a spiral magnetic field, *Geophys. Res. Lett., 28*, 223, 2001a.

Pierrard, V., M. Maksimovic, and J. Lemaire, Electronic velocity distribution function from the solar wind to the corona, *J. Geophys. Res., 104*, 17,021, 1999.

Pierrard, V., M. Maksimovic, and J. Lemaire, Core, halo and strahl electrons in the solar wind, *Astrophys. Space Sci.*, in press, 2001b.

Rosenbluth, M. N., W. McDonald, and D. L. Judd, Fokker-Planck equation for an inverse-square force, *Phys. Rev., 107*, 1, 1957.

Scudder, J. D., Why all stars should possess circumstellar temperature inversions, *Astrophys. J., 398*, 319, 1992.

Shizgal, B., and R. Blackmore, A discrete ordinate method of solution of linear boundary value and eigenvalue problems, *Journal of Computational Physics, 55*, 313, 1984.

Spitzer, L., *Physics of Fully Ionized Gases*, 105 pp., Wiley-Interscience, New York, 1956.

---

V. Pierrard and J. Lemaire, Institut d'Aéronomie Spatiale de Belgique, 3 Avenue Circulaire, B-1180 Brussels, Belgium. (viviane.pierrard@oma.be)

M. Maksimovic, DESPA, Observatoire de Paris, 92195 Meudon Cedex, France.

(Received April 17, 2001; revised August 17, 2001; accepted August 17, 2001.)